Scientific paper

Removal of Methyl Violet 2B and Direct Black 22 from Single and Binary System Using a Magnetic Zeolite/MgO/Starch/Fe_3O_4 Nanocomposite

Serap Fındık

Hitit University, Engineering Faculty, Chemical Engineering Department, Kuzey Yerleskesi, Çevre Yolu Bulvarı, 19030, Çorum, Türkiye

** Corresponding author: E-mail: serapfindik@hitit.edu.tr*

Received: 09-13-2023

Abstract

This study focuses on the preparation and characterization of magnetic zeolite (FSM-Zeo) using starch, magnesium oxide, and Fe_3O_4. Various analyses, including BET, FTIR, SEM, EDS, XRD, Zeta potential, and VSM, were conducted to assess the properties of FSM-Zeo. The adsorption capacity of FSM-Zeo was investigated for methyl violet (MV-2B) and direct black 22 (DB-22) in both single and binary dye solutions. Key parameters such as adsorbent amount, initial dye concentration, contact time, temperature, initial pH, and ionic strength were examined in the single system. Kinetic and isotherm studies revealed that DB-22 and MV-2B adsorption followed the pseudo-second-order model. Moreover, Freundlich and Langmuir models were confirmed for MV-2B and DB-22 adsorption on FSM-Zeo, respectively. In the binary system, the presence of MV-2B enhanced the adsorption of DB-22, resulting in higher removal compared to the single dye solution. A synergistic effect was observed due to the interaction between DB-22 and MV-2B, promoting the adsorption of DB-22 on FSM-Zeo.

Keywords: Adsorption; direct black 22; methyl violet 2B; magnetic zeolite; magnetite

1. Introduction

The dyes used in industries such as textiles, printing, plastics and paper have a complex aromatic structure. Among these industries, the textile industry is one of the largest consumers of water containing various dyes. If dye-containing wastewater is discharged into the receiving environment without treatment, it causes a decrease in photosynthesis and sunlight penetration. In addition, the dye in water produces toxic and harmful compounds through oxidation, hydrolysis or chemical reactions. These dyes are dangerous for humans, aquatic organisms and other living organisms due to their cancerogenic, mutagenic and toxic effects.[1,2] In order to eliminate the negative effects of the dye on the environment and living organisms, wastewater containing dyes must be treated before being discharged into the environment.

There are several treatment methods for the elimination of dyes from the wastewater such as chemical treatment (ozonation, photolysis, photocatalysis etc.), physicochemical treatment (adsorption, ion exchange, membran filtration etc.) and biological treatment (aerobic and anaerobic degradation). However, these methods have some limitations, including high operating costs, production of toxic by-products, generation of sludge, and disposal issues.[3] Amoung these methods, adsorption is the most suitable method due to its flexibility, simplicity, low cost, and absence of toxic sludge.[4] Adsorption is a mass transfer process in which a solid substance called adsorbent collects dissolved substances in aqueous solution on its surface. The efficiency of adsorption depends on various factors related to the adsorbent, including its molecular structure, molecular weight, surface area, particle size, cost, availability, and ease of use.[3] There are different types of adsorbents that can be used to remove dyes, such as agricultural wastes, industrial and urban wastes, clays, and natural polymers.[1]

Bio-adsorbents such as starch, lignin, chitosan, cellulose, and pectin are widely used due to their low cost, biodegradability and non-toxicity. Starch, which is one of the most abundant biopolymers, contains hydroxyl groups in its structure. However, starch has low mechanical strength, which can be improved through modification.[5,6] MgO is common-

ly used in polymer metal matrix composites because of its excellent heat resistance, good thermal properties, and high tensile strength.[7] Zeolite is a naturally abundant adsorbent with a porous structure consisting of crystalline alumina silicate. There are more than 40 types of naturally occurring zeolites, and clinoptilolite is one of the most abundant types with low cost and a high surface area. Zeolite can be used in its natural form or modified to enhance its adsorption capacity through thermal or chemical methods.[8]

The use of magnetic nanoparticles as adsorbents has been increasing due to their functional groups, active sites, adsorption capacity, surface area and easy of separation.[4] Among magnetic particles, iron oxides, such as magnetite (Fe_3O_4), hematite (α–Fe_2O_3), and maghemite (γ–Fe_2O_3), have garnered attention due to their ease of synthesis, magnetic susceptibility, biocompatibility, and low cost. Among these, Fe_3O_4 is the most extensively studied iron oxide. It can be easily modified, and new nanoadsorbents can be developed using low-cost conventional materials.[9]

Numerous studies in the literature have explored adsorbents incorporating clay, starch, and iron oxide for various applications. Noteworty examples include the removal of methyl violet using clay/starch/Fe_3O_4,[10] the removal of sunset yellow and Nile blue using clay/starch/$MnFe2O_4$,[5] the removal of methylene blue, methyl violet and crystal violet using clinoptilolite/starch/$CoFe_2O_4$,[11] the removal of methylene blue and methyl violet using Montmorillonite clay/starch/$CoFe_2O_4$,[1] and the removal of anionic Biebrich Scarlet using magnetic Fe_3O_4 zeolite 13X.[12] However, a significant gap exists in the literature regarding composites comprising starch, Fe_3O_4, MgO, and zeolite. This study introduces an environmentally friendly and novel magnetic adsorbent composed of zeolite, starch, MgO, and Fe_3O_4. The innovative composite shows promise for efficiently removing dyes from aqueous solutions, filling a critical research void, and demonstrating significant potential in advancing dye removal technologies.

In this study, a magnetic zeolite (FSM-Zeo) was prepared using starch, MgO and Fe_3O_4. The adsorption ability of FSM-Zeo was investigated for the removal of the cationic dye methyl violet (MV-2B) and the anionic dye direct black 22 (DB-22) in single and binary dye solutions. FSM-Zeo was characterized using various analyses such as SEM, EDS, XRD, BET, Zeta potential, VSM, and FTIR. The effects of adsorption parameters, including contact time, initial dye concentration, FSM-Zeo amount, ionic strength, temperature, and initial pH of the solution on the adsorption of DB-22 and MV-2B were studied. Additionaly, equilibrium and kinetic studies were performed.

2. Materials and Methods

2. 1. Materials

In the study, zeolite (a commercial product obtained from a company in Türkiye), $FeSO_4.7H_2O$ (Merck), $FeCl_3.6H_2O$ (Sigma Aldrich), $MgSO_4.7H_2O$ (Merck, 99 %), ethyl alcohol (Merck, 96 %) and starch (Carlo Erba, code 417587) were used to prepare magnetic composite. Adsorption experiments were performed using MV-2B (C.I. 42535, Isolab) and DB-22 (commercial name Direct Black 22 VSF 1600, supplied from a company named "HNY" in Turkey). All the chemicals were used without purification.

2. 2. Preparation of the Adsorbent and Characterization

The adsorbent used in the study was prepared using the chemical coprecipitation method.[5,10,13] Iron II sulphate heptahydrate ($FeSO_4.7H_2O$) and iron III chloride hexahydrate ($FeCl_3.6H_2O$) were dissolved in 100 mL of ethyl alcohol with a molar ratio of 1:1. The mixture was stirred for 10 minutes using a magnetic stirrer. $MgSO_4 \cdot 7H_2O$ was added to the iron solution and stirred for additional 10 minutes. Next, starch was added to the solution and stirred for 5 minutes. Zeolite was subsequently added to the solution and stirred for 30 minutes at a temperature of 70–75 °C. The weight ratio of starch to zeolite was 1:1. The pH of the solution was adjusted to 11 using 3 M NaOH solution. After adjusting the pH, stirring continued for one hour at a temperature of 75–80 °C. The prepared adsorbent was left overnight, washed several times with distilled water, and filtered using filter paper (Whatmann-40). Finally, it dried at 90 °C for 70 hours. The resulting adsorbent was coded as FSM-Zeo.

FSM-Zeo was characterized by BET (Quantachrome Nova Touch LX4), XRD (Bruker D8 Advence), FTIR (Bruker, Alpha), VSM (Lake Shore 7407), Zeta potential (Malvern ZetaSizer Nano ZSP), SEM and EDS (FEI, Quanta FEG250) analyses.

2. 3. Adsorption Experiments

In this study, process variables such as the contact time (0–90 min), initial pH (3.5–9), initial concentration of the dye solution (10–40 mg/L), NaCl amount (0.1–0.7 g/100 mL), Na_2SO_4 amount (0.1–0.7 g/100 mL), amount of adsorbent (0.1–0.5 g/100 mL) and temperature (22–50 °C) were investigated.

A known amount of FSM-Zeo was added to 100 mL dye solution with a known concentration and stirred at 300 rpm. Samples were taken from the dye solution and centrifuged at 3500 rpm for 10 minutes to separate the adsorbent. The concentrations of MV-2B and DB-22 were determined by measuring the absorbance of the sample using UV spectrophotometer (Hach, DR-2400). The absorbance of MV-2B was recorded at a wavelength of 584 nm, while the absorbance of DB-22 was measured at a wavelength of 481 nm. All the experiments were repeated at least three times.

The dye removal (R), was calculated using Eq. 1

$$R, \% = [(C_0 - C_t) / C_0]^*100 \quad (1)$$

The adsorption capacity of the FSM-Zeo at equilibrium (q_e, mg/g) was calculated using Eq. 2

$$q_e = \frac{(C_0 - C_e) * V}{W} \quad (2)$$

where V is the volume of the dye solution (L), W is the weight of the FSM-Zeo (g), C_0, C_t and C_e are the concentration of dye (mg/L) at initial, at any time and at equilibrium respectively.

3. Results and Discussion

3. 1. Characterization of the FSM-Zeo

The structure of FSM-Zeo and elemental distribution were examined using SEM-EDS analyses. Figure 1a and 1b show the SEM and EDS analyses of the zeolite (Z) and FSM-Zeo. In Figure 1a, the zeolite exhibits a porous, layered structure with a non-uniform surface. After the synthesis of FSM-Zeo, particles of various sizes can be observed on its surface, which can be attributed to the presence of Fe_3O_4, MgO, and starch. The weight percentages of the elements in Z and FSM-Zeo are presented in Table 1. The results indicate that FSM-Zeo has been successfully loaded with iron and magnesium. The BET specific surface area of Z and FSM-Zeo was determined as 16.79 m^2/g and 34.26 m^2/g respectively. These results indicate that the surface area of FSM-Zeo is enhanced compared to zeolite. Similar findings have been reported in the literature. For instance, Foroutan et al.[11] determined the surface area of clinoptilolite as 18.82 m^2/g in their study. Another study by Ahmedi et al.[1] reported the BET surface area of montmorillonite clay and the montmorillonite clay/starch/$CoFe_2O_4$ composite as 3.167 m^2/g and 27.27 m^2/g, respectively.

Figure 2 shows the XRD patterns of Z and FSM-Zeo. In the XRD diffraction pattern of Z, the main peaks observed at 2θ = 9.85°, 22.4°, 22.73°, 26.6°, 28.15°, 30.2° and 31.7° correspond to clinoptilolite (PDF#39-1383). In the XRD pattern of FSM-Zeo, the main peaks associated with clinoptilolite remained unchanged, suggesting the crystal structure of clinoptilolite remained stable during the synthesis process. Additionally, new diffraction peaks appeared in the FSM-Zeo XRD pattern at 30.19°, 35.8°, 43.3°, 57.5°, and 63.05°, which are characteristic peaks of magnetite (Fe_3O_4). These magnetite diffraction peaks are

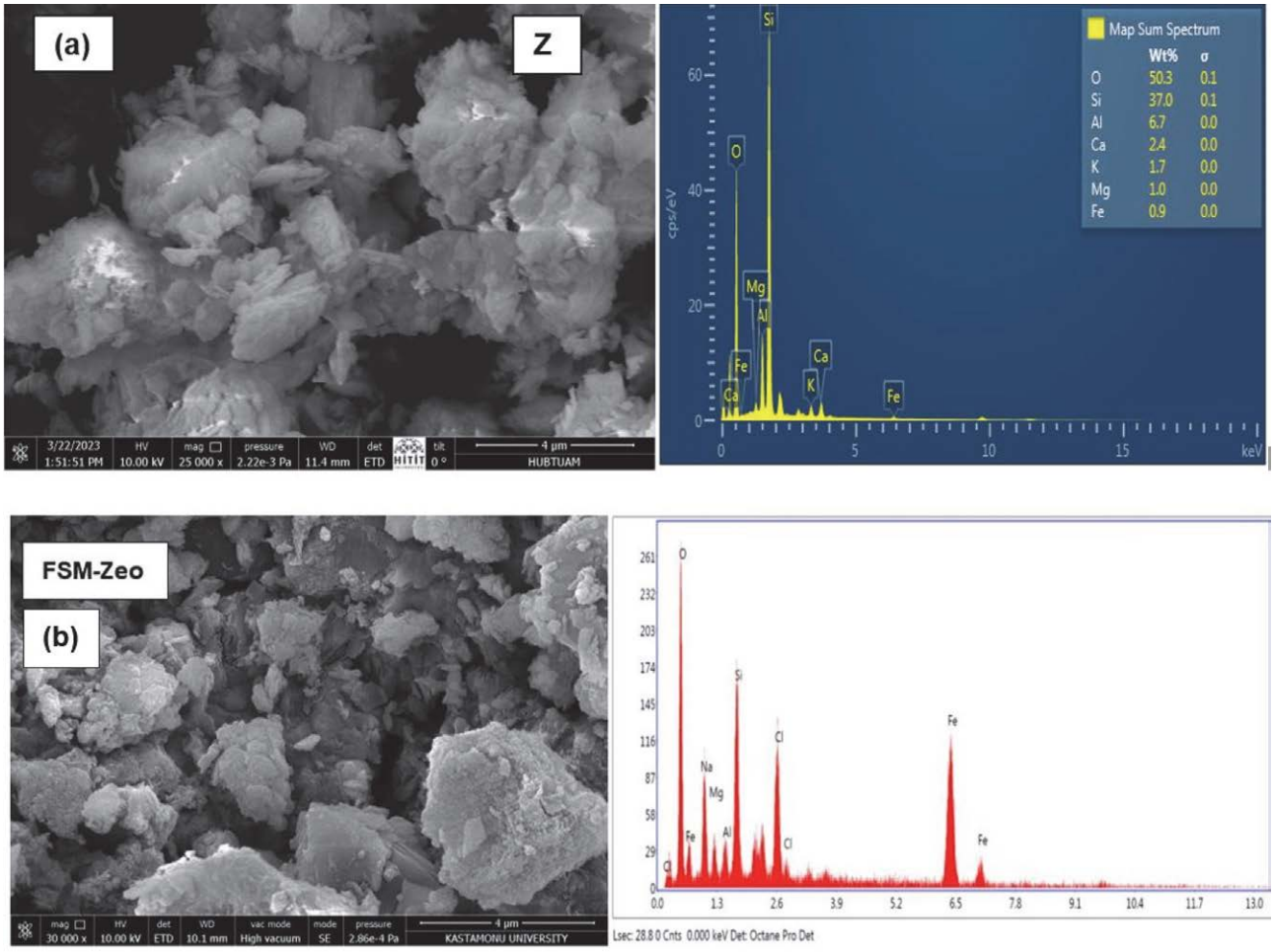

Fig. 1. The SEM and EDS spectra of (a) Z and (b) FSM-Zeo

Table 1. Results of the EDS analysis

Element	Z Weight (%)	FSM-Zeo Weight (%)
O	50.3	30.75
Si	37.0	9.4
Al	6.7	2.33
Ca	2.4	0.84
K	1.7	0.72
Mg	1	3.08
Fe	–	27.92
Cl	–	7.62
Na	–	13.40
S	–	3.93

in accordance with the PDF card 75–0449 and have been reported in previous studies.[14–16] Furthermore, a diffraction peak at 75.15° can be attributed to MgO, and it matches with the PDF card 45-0946.

The magnetization curve of FSM-Zeo exhibits a S-shaped curve, indicating superparamagnetic behavior. This behavior is characterized by zero coercivity and remanence at room temperature. The superparamagnetic properties of FSM-Zeo enable it to be easily separated from the dye solution using a magnet after the adsorption process. This magnetic separation capability has been reported in previous studies.[17,18]

Figure 3b presents the FTIR spectra of Z, FSM-Zeo, FSM-Zeo after the adsorption of MV-2B, DB-22, and MV-2B/DB-22. In the spectrum of Z, the peaks observed at 3395 cm^{-1} and 1632 cm^{-1} can be attributed to the hydroxyl (OH) groups present on the surface of clinoptilolites. These peaks indicate the presence of adsorbed water molecules.[8,11,19] The absorption peak at 1025 cm^{-1} corresponds to the stretching vibration of silicate groups in the structure of Z.[11,19] The absorption peaks at 450 cm^{-1} and 790 cm^{-1} indicate the vibrations of Si-O or Al-O bonds in the clinoptilolite structure.[11,19]

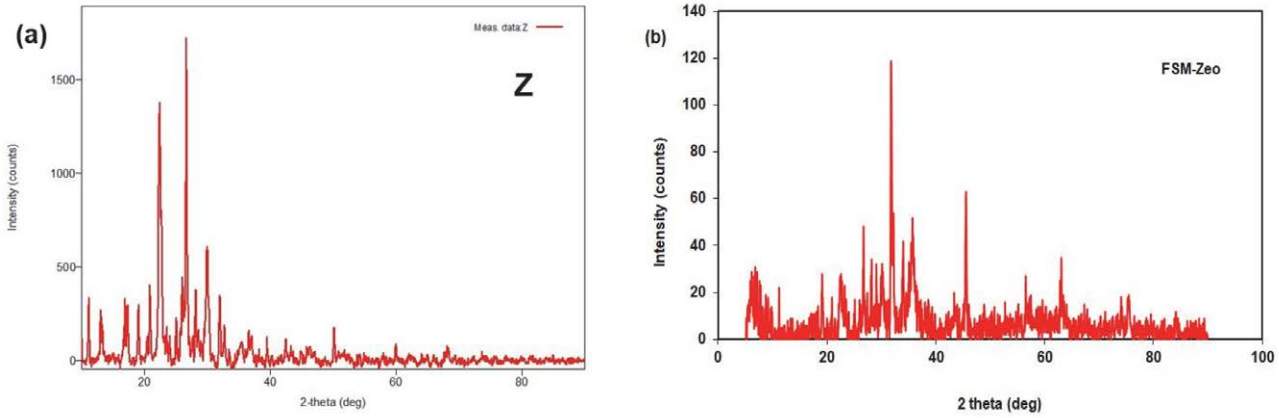

Fig. 2. (a) XRD analysis of Z and (b) FSM-Zeo

Figure 3a shows the VSM (Vibrating Sample Magnetometer) analysis of FSM-Zeo. The magnetic saturation value of FSM-Zeo was determined as 8.41 emu/g at room temperature under a magnetic field of ± 20000 Qe.

Similar peaks to Z were observed after the synthesis of FSM-Zeo, indicating a favorable interaction between starch and Fe_3O_4 in the FSM-Zeo structure. The peak at 605 cm^{-1} in FSM-Zeo corresponds to the Fe-O bond.[19] Fig-

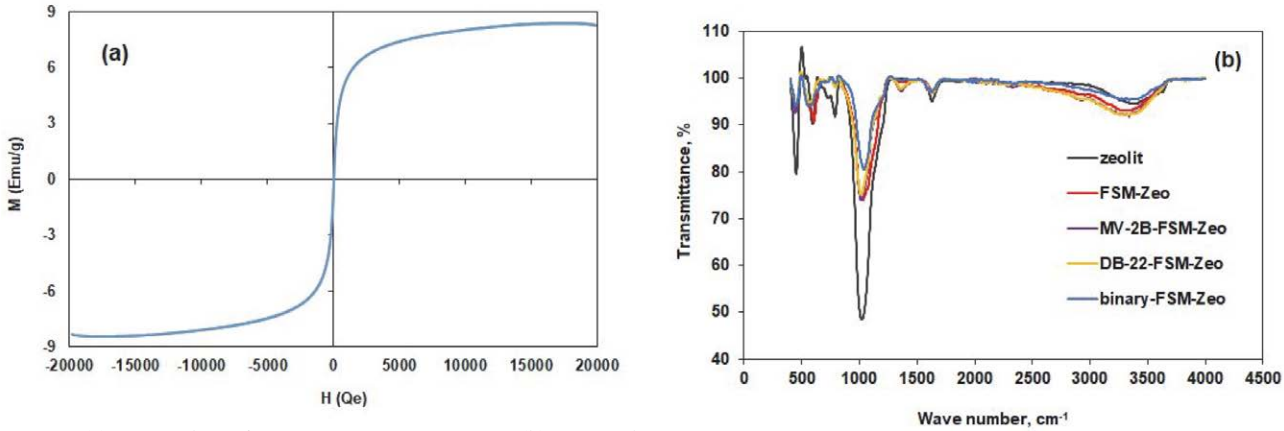

Fig. 3. (a) VSM analysis of FSM-Zeo at room temperature (b) FTIR analysis

ure 3b demonstrates that there are no significant changes in the peaks of FSM-Zeo before and after the adsorption of dyes. However there are changes in the peak intensities. The variations in the intensity of the bands after the adsorption of dyes onto FSM-Zeo may indicate the interaction of the dyes with the FSM-Zeo structure.[11]

3. 2. Effect of FSM-Zeo Amount

In the study, the effect of FSM-Zeo amount on the removal of MV-2B and DB-22 was investigated at 20 mg/L initial dye concentration, 22 °C temperature, original pH and 60 min contact time. Figure 4a shows the results. The removal of MV-2B and DB-22 increased from 45.5% and 20.8% to 62.2% and 61% with increasing FSM-Zeo amount from 0.1 g/100 mL to 0.4 g/100 mL respectively. After 0.4 g/100 mL, the removal rates of MV-2B and DB-22 slightly decreased to 61.2% and 60.2% respectively. Therefore, the optimum adsorbent amount was determined to be 0.4 g/100 mL under the studied conditions.

The increase in removal rate with the increasing amount of adsorbent can be attributed to the availability of more active sites and a sufficient specific surface area for the adsorption of dye molecules.[10,20] However, beyond the optimum adsorbent amount, there is no significant change in the removal of dyes. This could be due to the accumulation of the adsorbent particles, which may hinder the accessibility of dye molecules to active sites, resulting in a decrease in the active surface area available for adsorption.[21]

3. 3. Effect of Initial pH and Temperature

The effect of initial dye solution pH was examined in the range of 3.5–9. The original pH of the MV-2B and

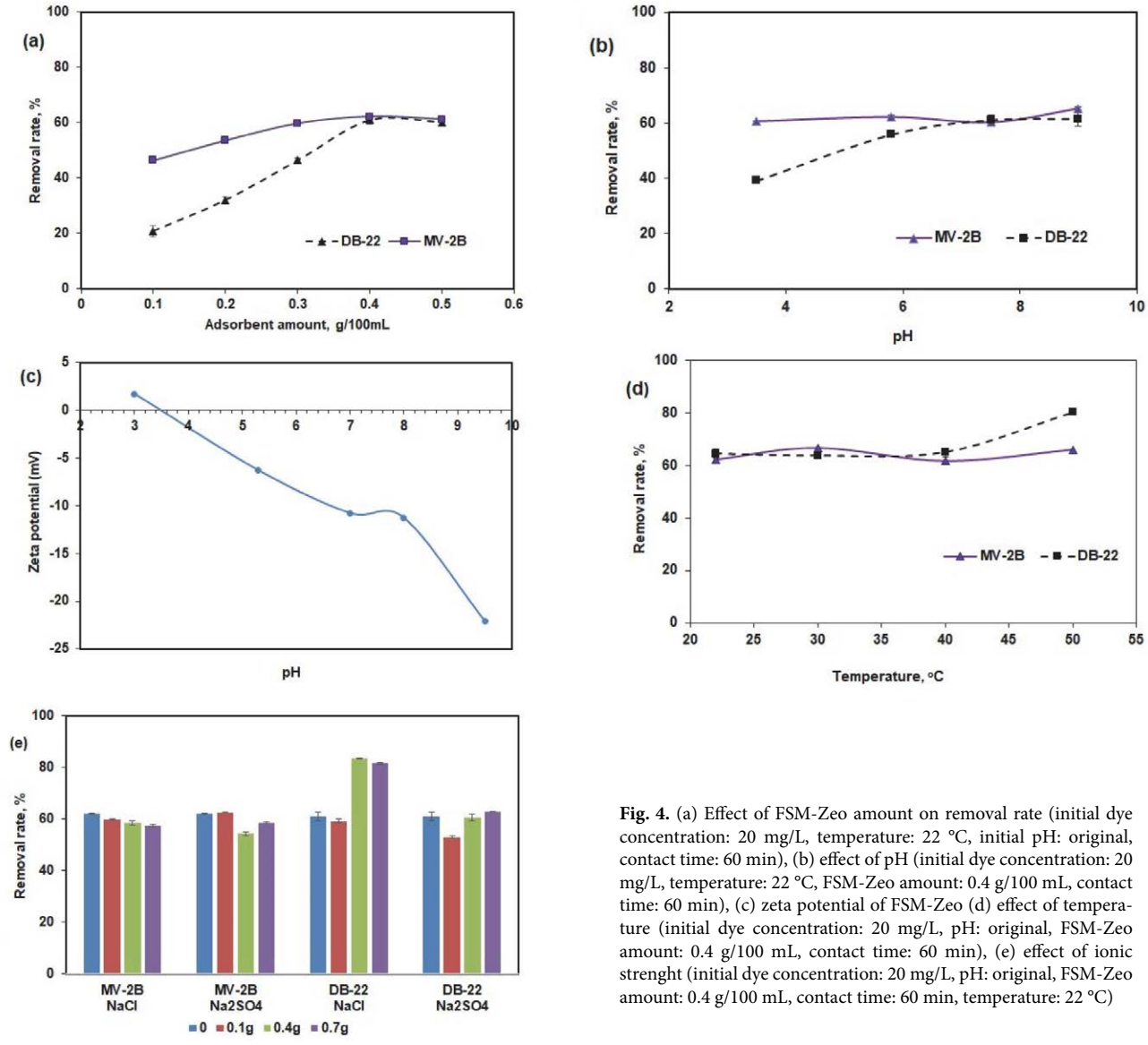

Fig. 4. (a) Effect of FSM-Zeo amount on removal rate (initial dye concentration: 20 mg/L, temperature: 22 °C, initial pH: original, contact time: 60 min), (b) effect of pH (initial dye concentration: 20 mg/L, temperature: 22 °C, FSM-Zeo amount: 0.4 g/100 mL, contact time: 60 min), (c) zeta potential of FSM-Zeo (d) effect of temperature (initial dye concentration: 20 mg/L, pH: original, FSM-Zeo amount: 0.4 g/100 mL, contact time: 60 min), (e) effect of ionic strenght (initial dye concentration: 20 mg/L, pH: original, FSM-Zeo amount: 0.4 g/100 mL, contact time: 60 min, temperature: 22 °C)

DB-22 solutions were 5.8 and 7.5 respectively. The pH of the dye solution was adjusted before starting the experiment. It was not controlled during the experiment. Figure 4b shows the effect of pH on dye removal. MV-2B removal was found to be 60.7%, 62.2%, 60.3%, and 65.3 at solution pH 3.5, 5.8, 7.5 and 9 respectively. There was no significant change on the removal rate of MV-2B between pH 3.5–7.5. At pH 9 removal rate of MV-2B increased to 65.3%. On the other hand, removal of DB-22 increased from 39.2% and 55.8% to 61% and 61.5 % with increasing pH from 3.5 to 9.

The point of zero charge (pH_{pzc}) refers to the pH at which the surface's electrical charge density becomes zero. In the adsorption process, the pH_{pzc} value provides information about the electrostatic interaction between the surface and solute.[22] When medium pH > pH_{pzc}, surface of the adsorbent has negative charges while when medium pH < pH_{pzc}, the adsorbent surface has positive surface charges.[22,23] Figure 4c displays the Zeta potential results of FSM-Zeo, indicating that the pH_{pzc} value for FSM-Zeo was determined to be 3.5.

Adsorption of MV-2B and DB-22 on the FSM-Zeo surface can be explained by various mechanism such as pore saturation, electrostatic interaction between the adsorbent surface and dye molecules, hydrogen bonding, and π–π interactions between functional grups of the adsorbent and dye molecules.[1,24] One of the effective mechanisms in removing MV-2B and DB-22 is the presence of pores and porosity in the adsorbent. SEM analysis confirms the presence of pores, providing sites for the adsorbing MV-2B and DB-22 molecules, the removal of these dyes might occur through the pore saturation mechanism.[1] The mechanism of MV-2B and DB-22 dye adsorption at different pH values may be explained as follows. MV-2B molecules dissociate in water, forming positively charged molecules. At pH > pH_{pzc}, an electrostatic attraction occurs between the positively charged MV-2B molecules and the negatively charged surface of FSM-Zeo. Between pH 3.5 and 7.5, the adsorption rate of MV-2B shows no significant change. As the pH increases to 9, the concentration of OH^- ions increases, leading to more dominant role for electrostatic interaction.[1] Below pH 3.5, the high concentration of H^+ ions increases the competition between dye molecules and H^+ ions for adsorption onto the surface of the adsorbent.[11] π–π interaction, hydrogen bonding and pore saturation may play a significant role in the adsorption of MV-2B at pH values below 3.5.[1] On the other hand, DB-22 is an anionic dye consisting of negatively charged molecules. At pH > pH_{pzc}, the negative charges on the surface of the adsorbent result in no electrostatic interaction between DB-22 and the surface of FSM-Zeo. However, above the pH_{pzc}, π–π interaction and the hydrogen bonding with FSM-Zeo may play dominant roles in the adsorption of DB-22.[24]

The effect of temperature on the adsorption of MV-2B and DB-22 was examined at temperatures of 22, 30, 40 and 50 °C at 20 mg/L initial dye concentration, original pH, 0.4 g/100 mL adsorbent amount and 60 min contact time. Figure 4d shows the results. For DB-22, there was no significant change in its removal with increasing solution temperature from 22 °C to 40 °C. The removal rates of DB-22 were found to be 64.7%, 63.7%, and 65% at 22 °C, 30 °C, and 40 °C respectively. However, at 50 °C, the removal of DB-22 increased to 80.2%. A similar observation was reported by Fındık[25] in a study on the adsorption of DB-22 using synthesized magnetic kaolin supported zinc ferrite. The decrease in solution viscosity with increasing temperature leads to enhanced mobility of the dye molecules, resulting in more interactions between the dye molecules and the free active sites on the FSM-Zeo surface.

On the other hand, the removal of MV-2B remained nearly constant with increasing temperature. The removal rates of MV-2B were found to be 62.2% , 66.5%, 61.7% and 65.8% at 22 °C, 30 °C, 40 °C and 50 °C respectively. The stable performance efficiency observed between 22–50 °C. In literature, Chung et al.[26] obtained similar results for the adsorption of methylene blue. They reported that the nearly constant removal rate indicated the adsorptive stability of the adsorbent under various temperature changes. Similarly, Kanwall et al.[27] investigated the effect of temperature on the adsorption of crystal violet using native clay and Cl pretreated clay, and they observed no significant change in crystal violet adsorption with increasing temperature. The removal rate remained unchanged at higher temperature due to stability of the adsorbent. Overall, the effect of temperature on the adsorption of MV-2B and DB-22 varied. While DB-22 exhibited increased removal at higher temperatures, MV-2B showed a stable removal rate across the temperature range studied.

3. 4. Effect of Co-Existing Ions

In the study, the effect of ionic strength on the removal of dye was investigated using NaCl and Na_2SO_4 at different amounts. Figure 4e shows the results. For MV-2B, the removal rate decreased with increasing NaCl amount. However, the addition of 0.1 g/100 mL Na_2SO_4 did not significantly affect the removal rate of MV-2B. At 0.4 g/100 mL and 0.7 g/100 mL Na_2SO_4 amounts, the removal rate of MV-2B was lower than without Na_2SO_4. This observation suggests that there is competition between ions and dye molecules to be adsorbed onto the FSM-Zeo surface. This phenomenon can affect the availability of active sites for dye adsorption.[11]

On the other hand, the removal of DB-22 decreased with the addition of 0.1 g/100 mL NaCl or Na_2SO_4, but the removal rate increased with increasing salt concentration. DB-22 removal rates were found to be 83.5% with addition of 0.4 g/100 mL NaCl and 61% without salt. In literature, Olesegun and Mohallem[28] observed that the adsorption of Congo red increased with increasing NaCl concentration. They suggested that the increase in removal rate may be attributed to enhanced hydrophobic interactions, which

lead to the shielding of intermolecular repulsion between the dye and the nanocomposite. The increase in removal rate with increasing salt concentration offers an advantage in treating textile wastewater that contains high levels of salt. Overall, it can be concluded that FSM-Zeo effectively removes DB-22 in the presence of NaCl and Na_2SO_4.

3. 5. Effect of Contact Time and Initial MV-2B Concentration

Figure 5 shows effect of the contact time and initial dye concentration on the removal of MV-2B and DB-22 using 0.4 g/100 mL FSM-Zeo amount at 22 ° C and original pH. The initial dye concentration was varied between 10–40 mg/L. The removal rates of MV-2B and DB-22 decreased from 73 % and 72 % to 51 % and 40.7% respectively, as the initial concentration increased from 10 mg/L to 40 mg/L. This decrease in removal efficiency can be attributed to the rapid saturation of active sites on FSM-Zeo and a reduction in the number of available active sites. The limited number of active sites on FSM-Zeo leads to a decrease in dye removal efficiency.[1,11]

The effect of contact time on dye removal was studied over a range of 5–90 minutes. The results show that initially, the removal of dyes was rapid, indicating the presence of suitable and unsaturated active sites for adsorption. However, after a contact time of 45 minutes, the removal rate reached a plateau, and further contact time did not significantly affect the removal efficiency. This observation is consistent with the findings reported by Foroutan et al.[11] in their study on the adsorption of methyl violet, crystal violet, and methylene blue onto clinoptilolite/starch/$CoFe_2O_4$.

range of 10–40 mg/L initial concentrations while the other factors were kept constant (temperature: 22 °C, initial pH: original, FSM-Zeo amount: 0.4 g/100 mL). The linear form of the Langmuir, Freundlich and Temkin models, and as well as the separation factor (R_L) for Langmuir isotherm are given in Table 2.[18,29,30]

When fitting different models to experimental data, it may not be sufficient to use only the R^2 value to compare these models. Evaluation can be made by using the sum of the squared errors (SSE) and the R^2 value together. SSE value can be calculated using Eq. 3.[29]

$$SSE = \sum(q_{cal} - q_{exp})^2 \quad (3)$$

where q_{cal} and q_{exp} are the calculated and experimental values of q, respectively.

The calculated parameters of the isotherm models for the adsorption of MV-2B and DB-22 are presented in Table 2. The Freundlich model provided the best fit for the adsorption of MV-2B with the highest correlation coefficient (R^2 = 0.9921) and lowest SSE value. On the other hand, the Langmuir isotherm model exhibited good fitting for the adsorption of DB-22 with a R^2 value of 0.9695 and SSE value of 0.27. Figure 6a and 6b show the linear forms of the Freundlich and Langmuir isotherms for the adsorption of MV-2B and DB-22, respectively.

These results indicate that the adsorption of MV-2B occurs on a heterogeneous surface while the adsorption of DB-22 takes place on a homogeneous surface. The R_L values for the adsorption process of MV-2B and DB-22 dyes were in the range of 0–1, which indicates that the adsorption process can be desirable.[4] The K_L values for the MV-2B and DB-22 adsorption onto FSM-

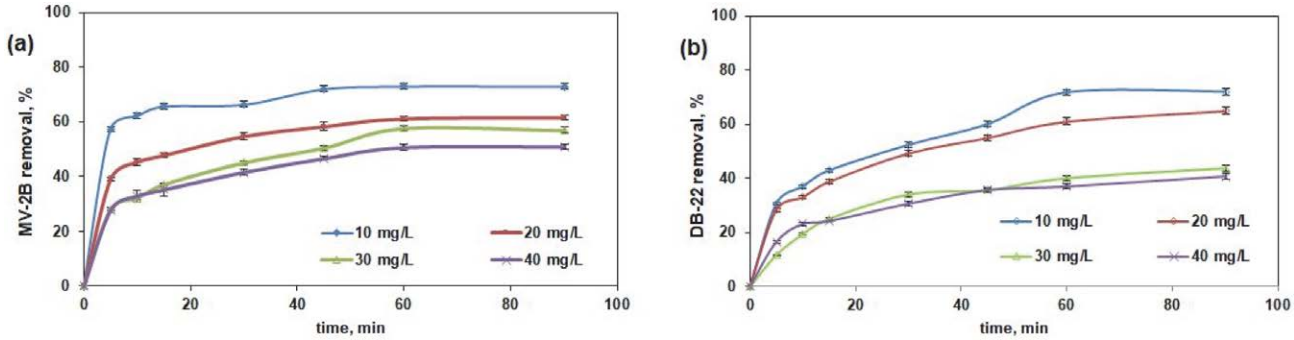

Fig. 5. Effect of initial concentration on the removal of (a) MV-2B (b) DB-22 (pH: original, FSM-Zeo amount: 0.4 g/100 mL, temperature: 22 °C)

3. 6. Adsorption Isotherms

The adsorption isotherm determines the interaction between the adsorbent and the adsorbate. That is, it is used to examine the relationship between the adsorbent and the dye it adsorbs.[11,29] The common isotherm models such as Langmuir, Freundlich and Temkin were applied to analyze adsorption of MV-2B and DB-22 onto FSM-Zeo in the

Zeo were determined as 0.117 L/mg and 0.276 L/mg, respectively. The higher K_L value for DB-22 suggests a stronger affinity between DB-22 molecules and the FSM-Zeo surface compared to MV-2B.[4] The Freundlich coefficient (n) for MV-2B and DB-22 adsorption were found to be 2.03 and 3.42, respectively. The value of n was greater than 1, it indicated that adsorption was physical and desirable.[4,5]

Table 2. Isotherm parameters for the adsorption of MV-2B and DB-22 (pH: original, FSM-Zeo amount: 0.4 g/100 mL, temperature: 22 °C)

Isotherm	Linear form of isotherm model	Constants	V-2B	DB-22
Langmuir	$\frac{ce}{q_e} = \frac{ce}{q_{max}} + \frac{1}{q_{max} K_L}$ $R_L = \frac{1}{(1 + K_L C_0)}$	q_{max} (mg/g)	7.16	4.43
		K_L (L/mg)	0.117	0.276
		R_L	0.18–0.43	0.083–0.24
		R^2	0.9777	0.9695
		SSE	0.12	0.27
Freundlich	$lnq_e = lnk_f + \frac{1}{n} lnC_e$	n	2.03	3.42
		K_f (mg/g)	1.178	1.574
		R^2	0.9921	0.8513
		SSE	0.056	0.33
Temkin	$q_e = \beta_1 lnK_T + \beta_1 lnC_e$	β_1	1.625	0.845
		K_T (L/mg)	1.069	4.279
		R^2	0.9733	0.8607
		SSE	0.139	0.28

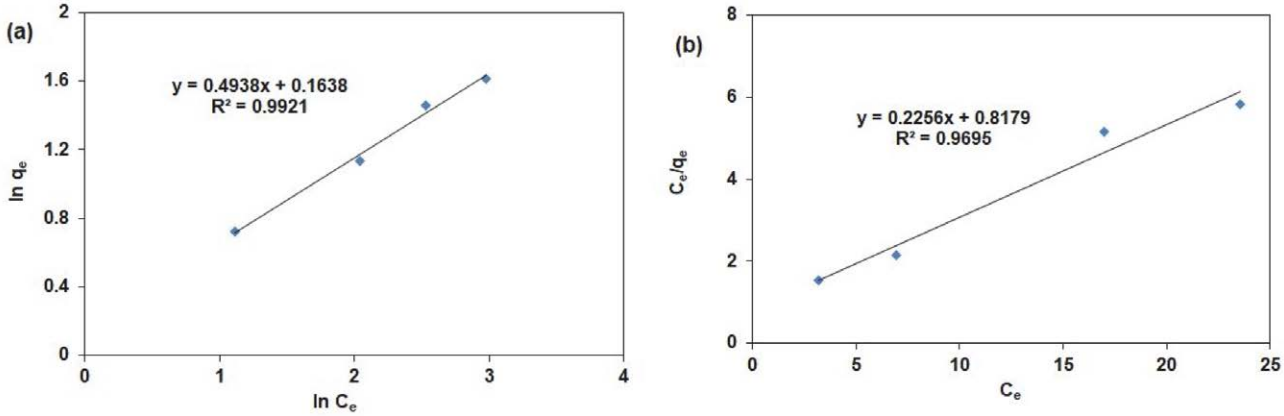

Fig. 6. Linear form of the (a)Freundlich isotherm for MV-2B and (b) Langmuir isotherm for DB-22 onto FSM-Zeo (pH: original, temperature: 22 °C, FSM-Zeo amount: 0.4 g/100 mL)

3. 7. Kinetic Analysis

The adsorption kinetic analysis of MV-2B and DB-22 onto FSM-Zeo was performed using common kinetic models such as pseudo first order (Ps.FO), pseudo second order (Ps.SO) and intraparticle diffusion models. The linear forms of these models[21] and the corresponding kinetic parameters obtained from the experimental data are presented in Table 3. The regression coefficient (R^2) value indicates the agreement between the calculated q_e values and the experimental q_e values obtained from the experiments. A higher R^2 value suggests a better fit of the kinetic model to the adsorption process. The results of the Ps.SO model and intraparticle diffusion model for MV-2B and DB-22 adsorption are shown in Figure 7.

According to Table 3, the Ps.SO model exhibited higher correlation coefficients (R^2 : 0.993–0.999 for MV-2B and R^2 : 0.988–0.998 for DB-22) compared to the Ps.FO model (R^2 : 0.715–0.939 for MV-2B and R^2 : 0.720–0.997 for DB-22). Additionally, there was a significant deviation between the calculated and experimental q values in the Ps.FO model, while the $q_{e,exp}$ and $q_{e,cal}$ values were closer in the Ps.SO model. These results indicate that the Ps.SO model provided the best fit for describing the adsorption kinetics of MV-2B and DB-22 on FSM-Zeo. In the Ps.SO model, the rate controlling step was determined to be a chemical reaction.[18]

As shown in Figure 7c and 7d, the relation of q_t against $t^{0.5}$ was linear. These results showed that the adsorption process was controlled by intraparticle diffusion mechanism. However, a deviation from linearity was observed within the 30–40 mg/L range, suggesting that adsorption on the layers surrounding the adsorbent influenced the overall adsorption process. Consequently, the intraparticle diffusion mechanism alone cannot fully account for the adsorption process at high initial dye concentrations.[21]

Table 3. Kinetic models constants for adsorption of MV-2B and DB-22 using the adsorbent FSM-Zeo (FSM-Zeo amount: 0.4 g/100 mL, pH: original, temperature: 22 °C)

Dye	Initial Conc. (mg/L)	$(q_e)_{Exp}$	Pseudo-first order $\ln(q_e-q_t) = \ln q_e - k_1 t$			Pseudo-second order $(t/q_t) = (1/k_2q_e^2) + (t/q_e)$			Intraparticle diffusion $q_t = k_p t^{1/2} + I$		
			k_1	q_e	R^2	k_2	q_e	R^2	k_p	I	R^2
MV-2B	10	2.06	0.0882	0.945	0.896	0.220	2.111	0.993	0.0606	1.557	0.880
	20	3.11	0.0647	1.832	0.939	0.069	3.264	0.999	0.1604	1.766	0.926
	30	4.30	0.1135	8.950	0.715	0.022	4.769	0.994	0.3342	1.438	0.957
	40	5.05	0.0975	6.758	0.783	0.026	5.459	0.997	0.3368	2.198	0.948
DB-22	10	2.04	0.0915	3.465	0.727	0.0349	2.316	0.988	0.1745	0.524	0.963
	20	3.22	0.0318	2.103	0.997	0.0246	3.532	0.994	0.2570	0.901	0.981
	30	3.29	0.0368	2.625	0.975	0.0155	3.858	0.998	0.3229	0.466	0.936
	40	4.05	0.0343	2.676	0.987	0.0203	4.450	0.995	0.3253	1.155	0.963

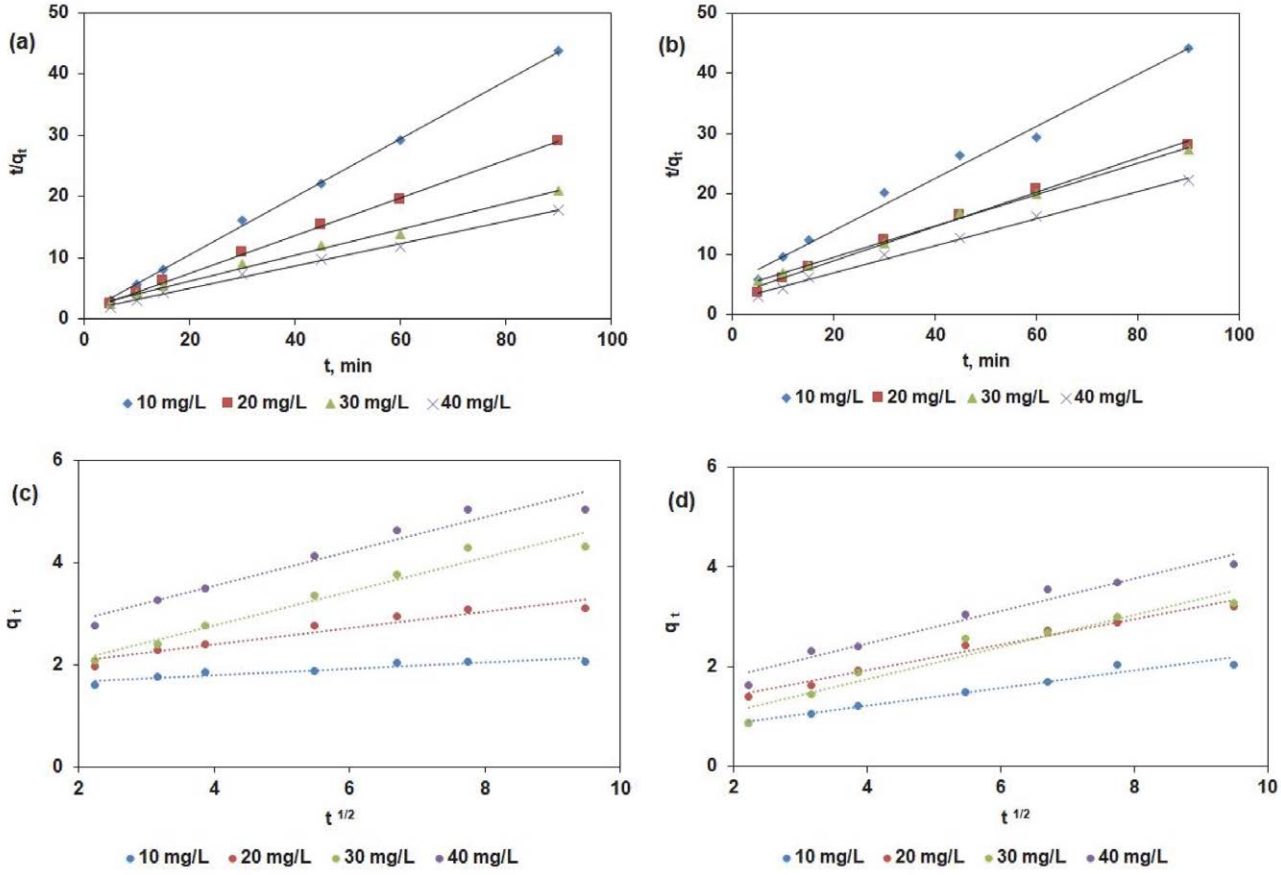

Fig. 7. Ps.SO model for the adsorption of (a) MV-2B, (b) DB-22 onto FSM-Zeo, intraparticle diffusion model for the adsorption of (c) MV-2B, (d) DB-22 onto FSM-Zeo

3. 8. Adsorption Studies on the Binary System

To investigate the adsorption of dyes in binary systems, a dye solution was prepared using DB-22/MV-2B with varying initial concentrations ratios such as 10/10, 10/20 and 20/10. The adsorption experiments for the binary system were performed using 0.4 g/100 mL of FSM-Zeo amount, at 22 °C and the original solution pH. The experimental studies followed the same procedure as for the single dye solution.

In binary systems the concentration of each dye was calculated using equations 4 and 5.[17,31]

$$C_A = \frac{k_{B2}{}^*A_1 - k_{B1}{}^*A_2}{k_{A1}{}^*k_{B2} - k_{A2}{}^*k_{B1}} \quad (4)$$

$$C_B = \frac{k_{A1}{}^*A_2 - k_{A2}{}^*A_1}{k_{A1}{}^*k_{B2} - k_{A2}{}^*k_{B1}} \quad (5)$$

Table 4. Removal of dyes and ratio of adsorption capacities in binary system

Initial dye concentration (mg/L)		Removal of dye (%)		R_q	
DB-22	MV-2B	DB-22	MV-2B	DB-22	MV-2B
10	0	72.0	–	–	–
20	0	65.0	–	–	–
0	10	–	73.0	–	–
0	20	–	61.7	–	–
10	10	85.6 59.9 97.9	1.05	0.73	
10	20	61.4		1.2	0.99
20	10	80.5	67.3	1.25	0.82

where A_1 and A_2 represent the total absorbance at wavelengths λ_{1max} and λ_{2max} and k_{A1}, k_{B1}, k_{A2}, k_{B2} are the calibration constants for components A and B at λ_{1max} and $\lambda_{2max.}$

The effect of both DB-22 and MV-2B dyes in binary system on removal performance of FSM-Zeo were determined using the ratio of adsorption capacities (R_q) as follows:[32,33]

$$R_q = q_{b,i}/q_{m,i} \quad (6)$$

where $q_{b,i}$ is the adsorption capacity for dye i in the binary system (mg/g) and $q_{m,i}$ is the adsorption capacity for dye i with the same initial concentration in a mono-component system. If $R_q > 1$, the adsorption of component i was enhanced by the other pollutant; if $R_q = 1$, the adsorption of component i was not affected by other pollutant; if $R_q < 1$, the adsorption of component i was suppressed by the other pollutant.

The effect of initial concentration on the removal of single dye solution and binary dye solution are presented in Table 4. The removal of DB-22 in binary dye solution was higher than the removal of DB-22 in single dye solution. The removal of DB-22 in binary dye solution found to be 85.6%, 97.9% and 80.5% at 10/10, 10/20 and 20/10 initial concentration of DB-22/MV-2B solution respectively. The ratio of adsorption capacities for DB-22 were higher than 1 at the studied conditions There was a synergistic effect due to the interaction between DB-22 and MV-2B, which promotes the adsorption of DB-22 on FSM-Zeo in binary systems. It means adsorption of DB-22 enhanced in the presence of MV-2B.

On the other hand, removal of MV-2B in binary dye solution found to be 59.9%, 61.4% and 67.3% at 10/10, 10/20 and 20/10 initial concentration of DB-22/MV-2B solution respectively. At 10/20 initial concentration of DB-22/MV-2B, the ratio of adsorption capacity for MV-2B was 0.99. It was very close to one and the presence of DB-22 in the solution did not effect the adsorption of MV-2B. R_q was 0.73 and 0.82 at 10/10 and 20/10 initial concentration of DB-22/MV-2B respectively. The R_q value showed that the presence of DB-22 suppressed the MV-2B adsorption at 10/10 and 20/10 initial concentration of DB-22/MV-2B.

In conclusion, considering the removal rates and R_q values in binary systems, it can be concluded that FSM-Zeo exhibited suitability for binary solutions under the investigated conditions. Furthermore, the results suggest that the adsorption of the anionic dye DB-22 from binary solutions is notably improved compared to the single-component system. In their study, Nicola et al.[17] investigated the removal of dyes from solutions containing both anionic and cationic dyes using magnetic mesoporous silica. In their work conducted at pH 4.5 and 6.3, they observed a decrease in the removal of the anionic dye Congo red (CR) and the cationic dye methylene blue (MB) compared to the single-component system. When comparing these results with the findings of this study, the obtained outcomes are advantageous for systems containing two dyes and for textile wastewater containing a high number of dyes.

3. 9. Comparison of FSM-Zeo with Other Adsorbents and Cost Analysis

The maximum adsorption capacity of the adsorbent depends on various parameters such as active surface sites, type of pollutants, modification methods, and precursor material of adsorbent.[5] Numerous studies have recently focused on developing low-cost adsorbents with high adsorption capacities. In this study, zeolite and starch biopolymer were utilized as cost-effective materials, while Fe_3O_4 and MgO were incorporated to gain magnetic properties and enhance the adsorption capacity of zeolite. The adsorption capacity of FSM-Zeo was compared to other adsorbents in existing literature (Table 5). FSM-Zeo exhibited a maximum adsorption capacity of 7.16 mg/g for MV-2B adsorption and 4.43 mg/g for DB-22 adsorption. Although magnetic property has gained with addition of Fe_3O_4 to zeolite, the maximum adsorption capacity remained relatively low. Moreover, it was observed that the higher amounts of adsorbent led to a lower adsorption capacities. Consequently, this study was limited to laboratory-scale experiments, and no investigations were carried out using real wastewater samples. Due to the low adsorption capacity of FSM-Zeo, it has no potential practical usage. However, the removal of DB-22 in binary dye solu-

tions demonstrated higher efficiency compared to single dye solutions, suggesting its usefulness in treating wastewater containing multiple dyes. Furthermore, the removal efficiency of DB-22 in single dye solution increases with an increase in the salt concentration, particularly with the addition of NaCl. Considering that NaCl is widely used in the textile industry, this is seen as an advantage. Further research can be conducted to improve the adsorption capacity of FSM-Zeo and reduce the required amount. The data obtained from this research may prove valuable to other researchers in the field.

Table 5. Comparison of the FSM-Zeo with other adsorbents

Adsorbent	Dye	Adsorbent amount (g/L)	Contact time (min)	q_{max} (mg/g)	References
Clay/starch/Fe_3O_4	Methyl violet	1.5	150	29.67	10
CLN/starch/$CoFe_2O_4$	Methylene blue	1.2	60	29.62	11
	Methyl violet	1.2	60	27.72	11
	Crystal violet	1.2	60	30.92	11
ZIF-8	Methylene blue	0.5	120	7.88	18
	Erichrome blackT	0.5	120	8.1	18
ACL/Fe_3O_4	Crystal violet	1.25	60	35.21	23
FSM-Zeo	MV-2B	4	90	7.16	This study
	DB-22	4	90	4.43	This study

The cost of FSM-Zeo includes raw materials, chemicals, and energy costs. This study aimed to minimize material costs by utilizing zeolite, a low-cost material. The magnetic adsorbent was synthesized using the co-precipitation method. When it comes to large-scale production of adsorbents, it is crucial to employ an easy preparation method and cost-effective materials in order to keep the adsorbent cost low. A recent study conducted by Augusto et al.[34] focused on the design, development, and economic analysis of large-scale plants for nanomagnetic materials used in environmental applications. Based on their literature review, they noted that the cost of magnetic nanoparticles can vary depending on their specific application, characteristics, and presentation form. For commercially available nanoparticles without any functionalization, the cost can range from $380 / kg (for iron oxides, including magnetite and maghemite) to $2255/kg (for nZVI).

4. Conclusion

In this study, a magnetic adsorbent called FSM-Zeo was synthesized and used for the adsorption of Direct black 22 (DB-22) and Methyl violet 2B (MV-2B) from both single and binary solutions. The structure of FSM-Zeo was characterized through analyzes such as BET, FT-IR, SEM, EDS, XRD, Zeta potential and VSM. The study investigated various adsorption parameters, including contact time, initial dye concentration, FSM-Zeo amount, NaCl amount, Na_2SO_4 amount, temperature, and initial pH of the solution for the adsorption of DB-22 and MV-2B. The results indicated that the adsorption of DB-22 and MV-2B followed the pseudo second order model. Isotherm studies showed that the adsorption of MV-2B and DB-22 onto FSM-Zeo followed Freundlich and Langmuir models, respectively. Notably, the study observed a trend of low adsorption capacity with a high adsorbent amount.

In the binary-dye system, the presence of MV-2B enhanced the adsorption of DB-22, leading to higher removal efficiency compared to the single-dye solution. Considering the dye removal rate and the ratio of adsorption capacities (R_q), it can be concluded that FSM-Zeo was effective in removing the DB-22/MV-2B mixture. Moreover, the removal efficiency of DB-22 in the single system increased with an increase in salt concentration, particularly with the addition of NaCl, presenting an advantageous aspect given the widespread use of NaCl in the textile industry. Further research is recommended to enhance the adsorption capacity of FSM-Zeo and reduce the required amount. The findings obtained from this research will contribute valuable insights to researchers in the field of dye adsorption.

Acknowledgement

The author thanks to Hitit University for their financial support of this project under contract of MUH19001.21.003.

5. References

1. A. Ahmadi, R. Foroutan, H. Esmaeili, S. J. Peighambardoust, S. Hemmati, B. Ramavandi, *Mat. Chem. Phys*. **2022**, *284*, 126088. **DOI:**10.1016/j.matchemphys.2022.126088
2. K. K. Kefeni, B. B. Mamba, T. A. M. Msagati, *Sep. Pur. Techn*. **2017**, *188*, 399–422. **DOI:**10.1016/j.seppur.2017.07.015
3. A. Kausar, M. Iqbal, A. Javeda, K. Aftab, Z. Nazli, H. N. Bhatti, S. Nouren, *J. Molec. Liq*. **2018**, *256*, 395–407. **DOI:**10.1016/j.molliq.2018.02.034

4. R. Foroutan, S. J. Peighambardoust, Z. Esvandi, H. Khatooni, B. Ramavandi, *J. Env. Chem. Eng.* **2021**, *9,* 104752. **DOI:**10.1016/j.jece.2020.104752
5 . Z. Esvandi, R. Foroutan, S. J. Peighambardoust, A. Akbari, B. Ramavandi, *Surf. Interfa.* **2020**, *21*, 100754. **DOI:**10.1016/j.surfin.2020.100754
6. S. S. Hosseini, A. Hamadi, R. Foroutan, S. J. Peighambardoust, B. Ramavandi, *J. Water Proc. Eng.* **2022**, *48,* 102911. **DOI:**10.1016/j.jwpe.2022.102911
7. Q. Yuan, H. Huang, W. Wang, G. Zhou, L. Luo, X. Zeng, Y. Liu, *J. Allo. Comp*. **2020**, *854*, 153889. **DOI:**10.1016/j.jallcom.2020.153889
8. A. Badeenezhad, A. Azhdarpoor, S. Bahrami, S. Yousefinejad, *Molec. Simul*. **2019**, *45,* 564–571. **DOI:**10.1080/08927022.2018.1564077
9. F. Mashkoor, A. Nasar, *J. Magnetis. Magnet. Mater*. **2020**, *500,* 166408. **DOI:**10.1016/j.jmmm.2020.166408
10. A. A. Mojarad, S. Tamjidi, H. Esmaeili, *Int. J. Env. Analyt. Chem*. **2022**, *102,* 8159–8180. **DOI:**10.1080/03067319.2020.1845665
11. R. Foroutan, S. J. Peighambardoust, S. Hemmati, H. Khatooni, B. Ramavandi, *Int. J. Biol. Macromol*. **2021**, *189*, 432 – 442. **DOI:**10.1016/j.ijbiomac.2021.08.144
12. A. A. AbdulRazak, Z. M. Shakor, S. Rohani, *J. Env. Chem. Eng.* **2018**, *6*, 6175–6183. **DOI:**10.1016/j.jece.2018.09.043
13. F. S. Ahmed, A. A. AbdulRazak, M. A. Alsaffar, *Materials Today: Proceed.* **2022**, *60*, 1676–1688. **DOI:**10.1016/j.matpr.2021.12.224
14. E. Altintig, A. Alsancak, H. Karaca, D. Angın, H. Altundag, *Chem. Eng. Comm.* **2021**, *209,* 555–569. **DOI:**10.1080/00986445.2021.1874368
15. A. Peyghami, A. Moharrami, Y. Rashtbari, S. Afshin, M. Vosuoghi, A. Dargahi, *J. Disp. Sci. Tech*. **2023**, *44,* 278–287. **DOI:**10.1080/01932691.2021.1947847
16. T. Huang, M. Yan, K. He, Z. Huang, G. Zeng, A. Chen, M. Peng, H. Li, L. Yuan, G. Chen, *J. Coll. Interf. Sci.* **2019**, *543*, 43–51. **DOI:**10.1016/j.jcis.2019.02.030
17. R. Nicola, S. G. Muntean, M. A. Nistor, A. M. Putz, L. Almasy, L. Sacarescu, *Chemosp.* **2020**, *261*, 127737. **DOI:**10.1016/j.chemosphere.2020.127737
18. M. Mahmoodi, V. Javanbakht, *Int. J. Biol. Macromol.* **2021**, *167*, 1076–1090. **DOI:**10.1016/j.ijbiomac.2020.11.062
19. M. Bayat, V. Javanbakht, J. Esmaili, *Int. J. Biol. Macromol.* **2018**, *116,* 607–619. **DOI:**10.1016/j.ijbiomac.2018.05.012
20. R. Foroutan, S. J. Peighambardoust, H. Aghdasinia, R. Mohammadi, B. Ramavandi, *Env. Sci. Poll. Res*. **2020**, *27,* 44218–44229. **DOI:**10.1007/s11356-020-10330-0
21. M. M. Boushehrian, H. Esmaeili, R. Foroutan, *J. Env. Chem. Eng.* **2020**, *8,* 103869. **DOI:**10.1016/j.jece.2020.103869
22. M. R. R. Kooh, M. K. Dahri, L. B. L. Lim, L. H. Lim, O. A. Malik, *Environ. Earth. Sci*. **2016**, *75*, 783. **DOI:**10.1007/s12665-016-5582-9
23. R. Foroutan, S. J. Peighambardoust, S. H. Peighambardoust, M. Pateiro, J. M. Lorenzo, *Molecules* **2021**, *26*, 2241. **DOI:**10.3390/molecules26082241
24. H. Kim, S. Kan, S. Park, H. S. Park, *J. Ind. Eng. Chem*. **2015**, *21*, 1191–1196. **DOI:**10.1016/j.jiec.2014.05.033
25. S. Fındık, *Acta Chim. Slov*. **2022**, *69,* 336–348. **DOI:**10.17344/acsi.2021.7289
26. J. Chung, N. Sharma, M. Kim, K. Yun, *J. Water Proc. Eng.* **2022**, *47*, 102763. **DOI:**10.1016/j.jwpe.2022.102763
27. A. Kanwal, H. N. Bhatti, M. Iqbal, S. Noreen, *Water Env. Res.* **2017**, *89,* 301–311. **DOI:**10.2175/106143017X14839994522984
28. S. J. Olusegun, N. D. S. Mohallem, *Env. Poll*. **2020**, *260*, 114019. **DOI:**10.1016/j.envpol.2020.114019
29. Z. Majid, A. A. AbdulRazak, W. A. H Noori, *Arab. J. Sci. Eng.* **2019**, *44,* 5457–5474. **DOI:**10.1007/s13369-019-03788-9
30. S. Sivalingam, S. Sen, *J. Taiw. Inst. Chem. Eng*. **2019**, *96,* 305–314. **DOI:**10.1016/j.jtice.2018.10.032
31. S. G. Muntean, M. A. Nistor, E. Muntean, A. Todea, R. Ianos, C. Pscurariu, *J. Chem*. **2018**, 6249821. **DOI:**10.1155/2018/6249821
32. J-H. Deng, X-R. Zhang, G-M. Zeng, J-L. Gong, Q-Y. Niu, J. Liang, *Chem. Eng. J*. **2013**, *226*, 189–200. **DOI:**10.1016/j.cej.2013.04.045
33. R. Tovar-Gómez, D. A. Rivera-Ramírez, V. Hernández-Montoya, A. Bonilla-Petriciolet, C. J. Durán-Valle, M. A. Montes-Morán, *J. Haz. Mat*. **2012**, *199–200*, 290–300. **DOI:**10.1016/j.jhazmat.2011.11.015
34. P. A. Augusto, T. Castelo-Grande, D. Vargas, A. Pascual, L. Hernández, A. M. Estevez, D. Barbosa, *Mater.* **2020**, *13*, 2477. **DOI:**10.3390/ma13112477

Povzetek

Študija je osredotočena na pripravo in karakterizacijo magnetnega zeolita (FSM-Zeo) z uporabo škroba, magnezijevega oksida in Fe_3O_4. Za oceno lastnosti FSM-Zeo so bile izvedene različne analize, vključno z BET, FTIR, SEM, EDS, XRD, Zeta potencialom in VSM. Adsorpcijska kapaciteta FSM-Zeo je bila raziskana za metil vijolično (MV-2B) in neposredno črno 22 (DB-22) v singularnih in binarnih raztopinah barvil. V singularnem sistemu so bili preučeni ključni parametri, kot so količina adsorbenta, začetna koncentracija barvila, kontaktni čas, temperatura, začetni pH in ionska moč. Kinetične in izotermne študije so pokazale, da je adsorpcija DB-22 in MV-2B sledila modelu psevdodrugega reda. Poleg tega sta bila Freundlichov in Langmuirjev model potrjena za adsorpcijo MV-2B oziroma DB-22 na FSM-Zeo. V binarnem sistemu je prisotnost MV-2B povečala adsorpcijo DB-22, kar je povzročilo večjo odstranitev v primerjavi z raztopino z enim barvilom. Opažen je bil sinergistični učinek zaradi interakcije med DB-22 in MV-2B, ki spodbuja adsorpcijo DB-22 na FSM-Zeo.